

Fig. 2. Cyclic voltammogram obtained during the reductive desorption of the oligopeptide. The current peaks for the oligopeptide (●) and L-cysteine (○) were  $-0.86$  V and  $-0.71$  V, respectively. Cyclic voltammograms were recorded at a scanning rate of  $20$  mV/s with respect to a Ag/AgCl reference electrode. The working electrode area was  $1.0$  cm<sup>2</sup>.

The chamber for perfusion culture (Fig. 1B) was fabricated with a poly(methyl methacrylate) plate using computer-aided laser machining (Laser PRO C180; GCC, Taiwan). The volume of the chamber was  $1.5$  mL. The chamber had three pairs of holes of  $800$   $\mu$ m in diameter at intervals of  $500$   $\mu$ m for the guidance of the gold rods. The gold rods with cells were fixed in the chamber, and  $1.5$  mL of the collagen solution was then poured into the chamber. After the gelation of the collagen, the rods were carefully extracted by applying a potential of  $-1.0$  V for  $5$  min. Then the chamber was connected to a microsyringe pump and culture medium was perfused at  $10$   $\mu$ L/min. To accelerate spontaneous vascularization, PMA was added to the culture medium to give a final concentration of  $20$  ng/mL [14,15].

## 2.7. Scanning electron microscopy

To observe cells on the gold rods under a scanning electron microscope (SEM), the culture was washed with PBS thrice and fixed with a mixed solution of  $2.5\%$  glutaraldehyde and  $2\%$  formaldehyde in PBS for  $1$  h at room temperature. Then, the culture was washed with PBS and fixed with  $1\%$  osmium tetroxide in PBS for  $1$  h at  $4^\circ$ C. The culture was washed with purified water and dehydrated with a graded ethanol series from  $30\%$  to  $90\%$  on ice and absolute ethanol substitution three times at room temperature. The solution was further substituted with  $100\%$  *t*-butanol, which was frozen at  $4^\circ$ C and dried by vacuum freeze-drying. The cells were observed under a SEM (ED-SEM; JEOL, Japan) operated at  $5$  kV.

## 3. Results and discussion

### 3.1. Electrical potential required for desorption of the oligopeptide

The amount of oligopeptide adsorbed on the gold surface was estimated to be  $8.7 \pm 1.4$  ng/cm<sup>2</sup> from three independent measurements with a QCM. This value corresponds to  $159$  pmol/cm<sup>2</sup>, which is high enough for the adhesion of cells (typical cases have required a maximum of  $\sim 20$  pmol/cm<sup>2</sup>) [16]. Cyclic voltammetry showed that the peak potentials for reductive desorption of the oligopeptide and cysteine were approximately  $-0.86$  V and  $-0.70$  V, respectively (Fig. 2). The relationship between the molecular configurations and the peak potentials required for cleaving the gold–thiolate bonds has been previously discussed in detail in experiments involving self-assembled alkanethiol monolayers [17,18]. The shape and potential of the peak are considered to be closely associated with a van der Waals interaction between the adsorbed molecules and the steric structure of the molecules [19,20]. As seen in Fig. 2, the peak for the oligopeptide is wider than that for cysteine, suggesting that the oligopeptide formed a relatively loose layer on the surface and had weak interactions with neighboring oligopeptides, probably because of its bulky structure. In general, the number of adsorbed molecules can be estimated from both the peak area in a cyclic voltammogram and by using a QCM. The amount of oligopeptide estimated by using a QCM was five times greater than that determined from the cyclic voltammogram. This fact suggests that the oligopeptide possibly

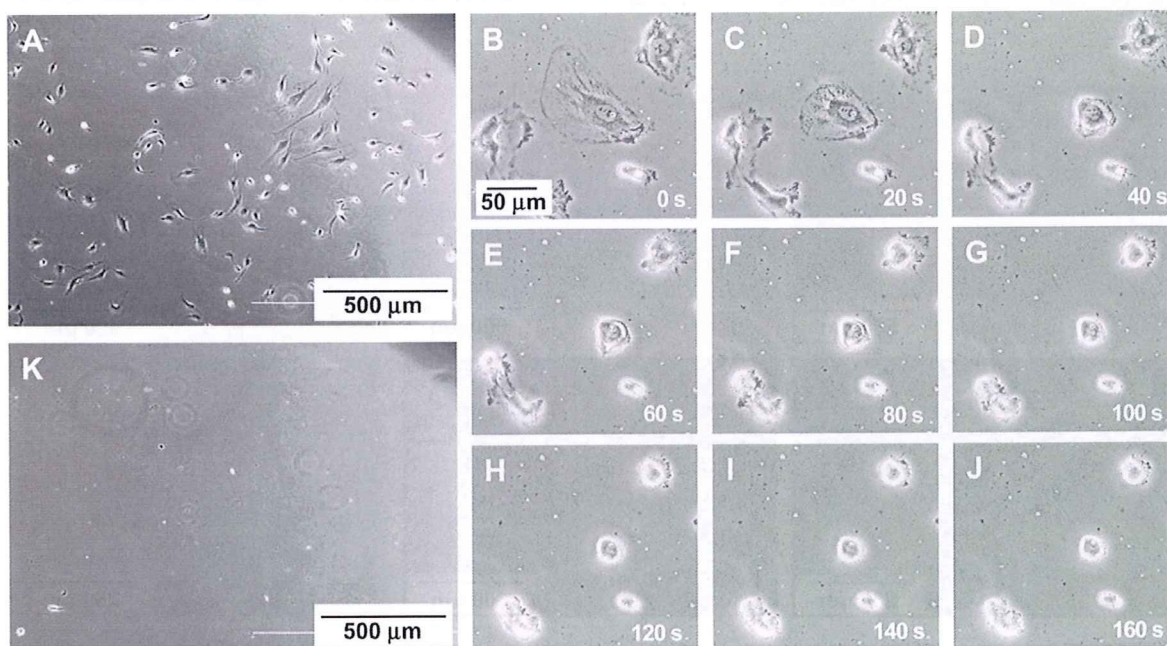
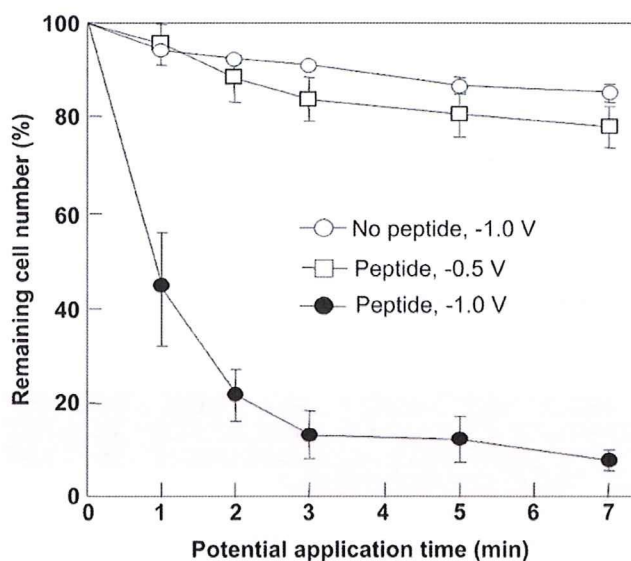


Fig. 3. Detachment of HUVECs from the gold surface. (A) Cells were readily attached to the gold surface modified with the oligopeptide during culturing for  $12$  h. (B–J) The change in cell morphology during the application of the electrical potential was observed at  $20$ -s intervals. The cells were gradually detached from the adhesive ends and appeared bright and round after the application of the potential. (K) The cells were withdrawn into a micropipette and found to be detached.





**Fig. 4.** Change in the number of HUVECs remaining on the gold surfaces. Approximately 90% of cells were detached within 7 min along with the desorption of the oligopeptide (●). Few cells detached from the surface in the absence of the oligopeptide (i.e., cells were directly attached to a gold surface [○]) or in application of a potential of  $-0.5$  V, which is smaller than that required to cleave the gold–thiolate bond (□). The error bars indicate SD calculated from nine independent experiments for each plot.

forms intermolecular cross-links via disulfide binding, and a part of the thiol group bonds to the gold surface. Although the details of the surface chemistry are still unclear, on the basis of the results that the oligopeptide desorbed in the potential range of  $-0.8$  to  $-1.0$  V,  $-1.0$  V was used for detachment of cells in the subsequent experiments.

### 3.2. Change in HUVEC morphology during cell detachment

HUVECs were readily attached via the oligopeptide and spread out on the gold surface (Fig. 3A). There was no significant

difference in the number of cells attached onto the gold surface with or without modification with the oligopeptide ( $1.0$ – $1.5 \times 10^4$  cells/cm<sup>2</sup>). At 18 h of culture, the cells attached onto the gold surface with the oligopeptide were detached by applying a potential of  $-1.0$  V. Fig. 3B–J shows the change in HUVEC morphology at 20-s intervals during the detachment. The cells were gradually detached from the adhesive ends and appeared bright and round after the application of the potential. These cells were identified to be detached after gentle pipetting (Fig. 3K).

To quantitatively analyze the detachment, the number of cells that remained on the surface was counted at 1, 2, 3, 5, and 7 min after the application of the potential (Fig. 4). When the oligopeptide and an electrical potential of  $-1.0$  V were used, more than 90% of the cells detached from the surface within 7 min. On the other hand, the behavior of the cells was clearly different in the control experiments (conditions of no oligopeptide or application of a potential of  $-0.5$  V, which is smaller than that required to cleave the gold–thiolate bond). These results suggest that cell detachment occurs mainly due to the electrically dependent desorption of the oligopeptide.

There are a few reports regarding the electrochemical detachment of cells. A self-assembled monolayer with electroactive sites that respond to electrical potentials has been used for micro-patterning of cells by detachment of cells from a selective region [21]. We have also previously shown that cells or cell sheets on the gold surface modified with alkanethiol could be detached by application of a potential [10]. To promote the adhesion of cells, the carboxyl terminal of alkanethiol has been coupled with an RGD peptide through carbodiimide-mediated cross-linking. Multilayered polyelectrolyte films formed by layer-by-layer deposition have also been used to detach cell sheets [22]. In this approach, the application of the relatively large potential,  $-1.8$  V, induces electrolysis of water and a local pH change, leading to the dissolution of the polyelectrolyte film and the detachment of cell sheets. An unsolved issue in these previous approaches is that molecules and other chemicals may be contained in the detached tissues and potentially could cause inflammatory responses in the body after transplantation. To alleviate this problem, we used an oligopeptide in this study. Since the oligopeptide contains an RGD sequence and spontaneously bonds to

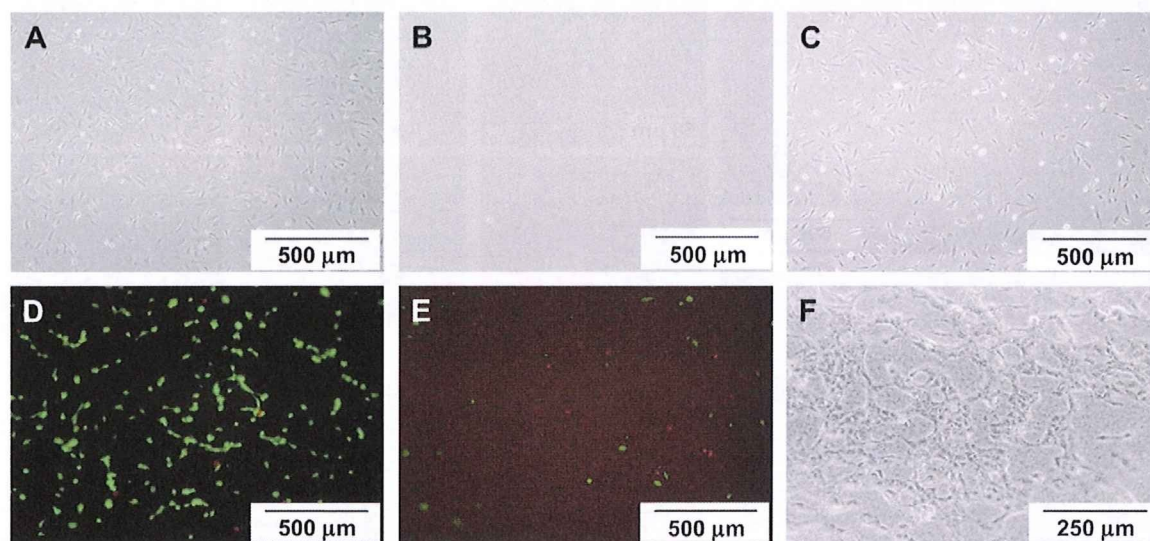


**Fig. 5.** Transfer of HUVECs to a collagen gel. Cells that attached to the gold surface modified with the oligopeptide (A) were transferred to a collagen gel, and few cells remained on the surface after potential application and peeling off the gel (B). Most of the cells remained attached on the gold surface that was not modified with the peptide even after the same potential was applied and the gel was peeled off (C). The cells transferred to the gel were viable, and few cells that were attached onto the surface modified with the peptide died (D), whereas only few cells that were attached onto the surface without peptide modification were transferred to the gel (E). The transferred cells grew and spread out on the gel at 1 day of culture (F).



a gold surface, the culture surface could be prepared without the use of coupling agents, simply by immersing a gold-coated substrate in a peptide solution. This may be advantageous for the widespread use of this technology in biological and medical laboratories.

### 3.3. Transfer of cells from the gold surface to collagen gel

After the collagen solution was poured and gelled on HUVECs on the gold surface with or without modification with the oligopeptide, a potential of  $-1.0$  V was applied for 5 min and the gel layer was peeled off. The cells that were attached to the gold surface with the oligopeptide were transferred to the gel, whereas in the case where the oligopeptide was not used only a few cells were transferred. Fig. 5B and C shows the surface of the substrates after peeling off the gel when the oligopeptide was and was not used, respectively. We then evaluated the viability of the transferred cells

in the gel by staining live cells with FDA (green) and dead cells with EB (red). Although the gelation may have trapped the cells in proximity to the electrode surface during the potential application, almost all the cells transferred were viable and few dead cells were observed in the gel (Fig. 5D). In the absence of the oligopeptide, only a small number of cells were transferred to the gel, some of which were dead cells (Fig. 5E). Fig. 5F shows the cells cultured for 24 h after the transfer into the gel. The cells grew and formed connections with each other on the gel. These results show that this approach (using an electrochemical reaction) can be used to transfer cells to the collagen gel noninvasively.

### 3.4. Fabrication of capillary-like structures in collagen gel

We applied this approach for the fabrication of capillary-like structures by transferring cells from thin gold rods to the inner

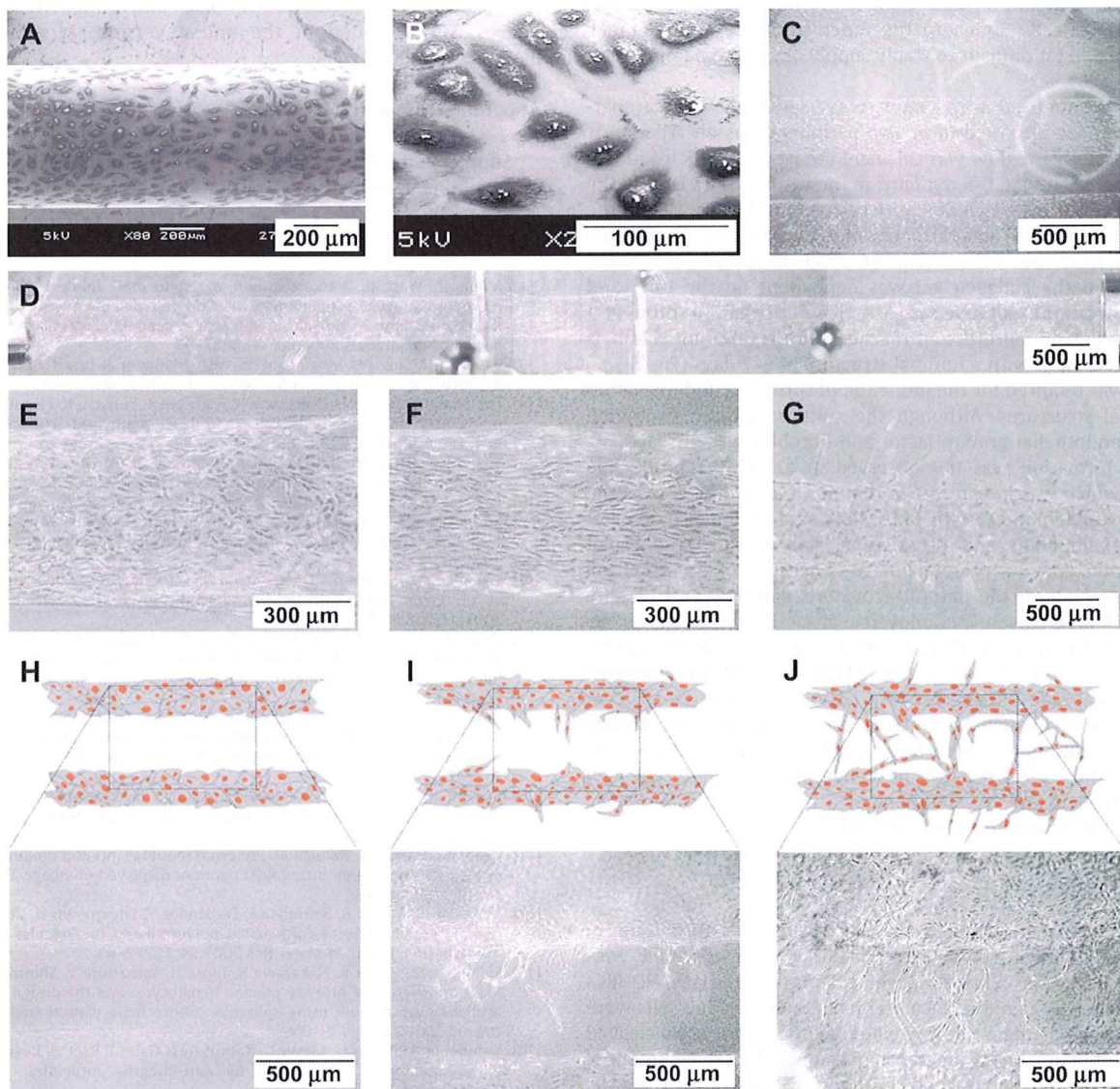


**Fig. 6.** Fabrication of capillary-like structures in collagen gel and formation of vascular networks. HUVECs were attached to the gold rod via the oligopeptide and grown to reach confluence at 3 days of culture (A, B). The capillaries were formed at ~500-μm intervals in a collagen gel (C). HUVECs were transferred throughout the capillaries (16-mm length) from the inlet to the outlet (D). The transferred HUVECs (E) oriented in the direction of the stream at 6 h of perfusion culture (F). HUVECs began to partly migrate into the collagen gel as early as 48 h (G). For the most part, HUVECs grew to form a dense cell layer on the surface at 2 days (H), and began to migrate into the collagen gel at ~4 days (I). At ~7 days, the luminal structures extended to the neighboring channels and bridged them (J).



surface of capillaries in a collagen gel (Fig. 1B). The rods covered with HUVECs (Fig. 6A and B) were aligned in the chamber and a collagen solution was poured and allowed to form a gel. After applying a potential of  $-1.0$  V for 5 min, the rods were carefully extracted from the chamber through guide holes, resulting in the formation of capillaries enveloped with HUVECs. The capillaries were formed at  $\sim 500$ - $\mu\text{m}$  intervals (Fig. 6C) and were 16 mm in length (Fig. 6D).

The guide holes were then connected to silicone tubes and the culture medium containing PMA was perfused through the capillaries at a flow rate of  $10 \mu\text{L}/\text{min}$ . Although the perfusion of culture medium was not necessarily required for oxygen supply in this experiment, when parenchymal cells such as hepatocytes are seeded in the collagen, a prompt initiation of culture medium flow will be required to satisfy their oxygen demand. Another approach was reported wherein a channel structure was constructed in a collagen gel and endothelial cells were then seeded into it to form a capillary-like structure. However, that approach required that the flow of culture medium was stopped for a while and the device was rotated to let cells attach to the inner surface of the channel, thereby making it difficult to stably supply oxygen to parenchymal cells [23].

The flow rate used in this study was relatively low in comparison with those observed in *in vivo* peripheral vessels. The shear stress caused by the flow was calculated to be  $0.12 \text{ dyn}/\text{cm}^2$  in this study, whereas it was  $1$ – $5 \text{ dyn}/\text{cm}^2$  in the venules [24]. During the perfusion culture, the HUVECs were oriented in the direction of the stream at 6 h (Fig. 6F) and partly began to migrate into the collagen gel at 48 h at the earliest (Fig. 6G). The formation of luminal structures in the collagen gel was dependent on the time and position. In a representative case, the HUVECs began to sprout at 4 days of perfusion culture, and reached the neighboring channels and bridged them with a luminal structure at  $\sim 7$  days (Fig. 6J).

PMA was required for the induction of sprouting and formation of luminal structures. Although the culture medium contained vascular endothelial growth factor and fibroblast growth factor-B, capillary formation was not observed in a highly reproducible manner, which was in contrast to that observed in the case of the medium supplemented with PMA. PMA is a potent promoter of tumor development and progression and activates the signal transduction enzyme protein kinase C because of its structural similarity to one of the natural activators, diacylglycerol [25,26]. Although PMA is currently employed in phase-I clinical trials for the treatment of patients with hematologic cancer or bone marrow disorder [27], its use should be avoided to prevent the development of its clinical side effects. Because HUVECs are known to form capillaries in a collagen gel when cultured in medium containing the abovementioned growth factors, optimization of the concentrations of these growth factors or their embedment in the collagen gel may lead to the development of a more suitable approach, which will eliminate the need for PMA.

#### 4. Conclusion

This study demonstrated an electrochemical technique to fabricate capillaries whose internal surface was covered with vascular endothelial cells in collagen gel. In this approach, HUVECs were attached to a gold surface via an oligopeptide. The cells were detached by applying a negative potential that reductively cleaved the gold–thiolate bonds. This technique allowed for detachment of more than 90% of the attached cells within 7 min of applying the negative potential, and could be used to detach cells not only from flat surfaces but also from thin rods. To fabricate the capillaries, a gold rod enveloped with HUVECs was inserted into a collagen gel. The rod was then extracted by applying a potential of  $-1.0$  V,

resulting in the formation of a capillary, which was enveloped with endothelial cells, in the collagen gel. During the subsequent perfusion culture, luminal structures were formed from the HUVECs lining the capillary and they bridged the neighboring capillaries to each other. This approach has potential for engineering vascularized tissues capable of delivering oxygen and nutrients to the entire tissue construct.

#### Acknowledgments

This research has been supported by MEXT (Grant-in-Aid for Young Scientists (A), 20686056), Ministry of Health, Labor and Welfare (H20-Saisei-wakate-010), and NEDO (Industrial Technology Research Grant Program, 06A06014a).

#### Appendix

Figures with essential colour discrimination. Figs. 5, and 6 of this article are difficult to interpret in black and white. The full colour images can be found in the online version, at doi:10.1016/j.biomaterials.2009.11.104

#### Appendix. Supplementary data

Supplementary material associated with this article is available in the online version at doi:10.1016/j.biomaterials.2009.11.104

#### References

- [1] Moon JJ, West JL. Vascularization of engineered tissues: approaches to promote angiogenesis in biomaterials. *Curr Top Med Chem* 2008;8(4):300–10.
- [2] Khademhosseini A, Langer R. Microengineered hydrogels for tissue engineering. *Biomaterials* 2007;28(34):5087–92.
- [3] Patel ZS, Mikos AG. Angiogenesis with biomaterial-based drug- and cell-delivery systems. *J Biomater Sci Polym Ed* 2004;15(6):701–26.
- [4] Fukuda J, Mizumoto H, Nakazawa K, Kajiwara T, Funatsu K. Hepatocyte organoid culture in elliptic hollow fibers to develop a hybrid artificial liver. *Int J Artif Organs* 2004;27(12):1091–9.
- [5] Richardson TP, Peters MC, Ennett AB, Mooney DJ. Polymeric system for dual growth factor delivery. *Nat Biotechnol* 2001;19(11):1029–34.
- [6] Lu YX, Shansky J, Del Tatto M, Ferland P, Wang XY, Vandenberg H. Recombinant vascular endothelial growth factor secreted from tissue-engineered bioartificial muscles promotes localized angiogenesis. *Circulation* 2001;104(5):594–9.
- [7] Levenberg S, Rouwkema J, Macdonald M, Garfein ES, Kohane DS, Darland DC, et al. Engineering vascularized skeletal muscle tissue. *Nat Biotechnol* 2005;23(7):879–84.
- [8] Croll TI, Gentz S, Mueller K, Davidson M, O'Connor AJ, Stevens GW, et al. Modelling oxygen diffusion and cell growth in a porous, vascularising scaffold for soft tissue engineering applications. *Chem Eng Sci* 2005;60(17):4924–34.
- [9] Chen X, Aledia AS, Ghajar CM, Griffith CK, Putnam AJ, Hughes CC, et al. Prevascularization of a fibrin-based tissue construct accelerates the formation of functional anastomosis with host vasculature. *Tissue Eng Part A* 2009;15(6):1363–71.
- [10] Inaba R, Khademhosseini A, Suzuki H, Fukuda J. Electrochemical desorption of self-assembled monolayers for engineering cellular tissues. *Biomaterials* 2009;30(21):3573–9.
- [11] Healy JM, Haruki M, Kikuchi M. Preferred motif for integrin binding identified using a library of randomized RGD peptides displayed on phage. *Protein Pept Lett* 1996;3(1):23–30.
- [12] McMillan R, Meeks B, Bensebaa F, Deslandes Y, Sheardown H. Cell adhesion peptide modification of gold-coated polyurethanes for vascular endothelial cell adhesion. *J Biomed Mater Res* 2001;54(2):272–83.
- [13] Fukuda J, Sakiyama R, Nakazawa K, Ijima H, Yamashita Y, Shimada M, et al. Mass preparation of primary porcine hepatocytes and the design of a hybrid artificial liver module using spheroid culture for a clinical trial. *Int J Artif Organs* 2001;24(11):799–806.
- [14] Gamble JR, Matthias LJ, Meyer G, Kaur P, Russ G, Faull R, et al. Regulation of *in vitro* capillary tube formation by anti-integrin antibodies. *J Cell Biol* 1993;121(4):931–43.
- [15] Montesano R, Orci L. Tumor-promoting phorbol esters induce angiogenesis *in vitro*. *Cell* 1985;42(2):469–77.
- [16] Houseman BT, Mrksich M. The microenvironment of immobilized Arg-Gly-Asp peptides is an important determinant of cell adhesion. *Biomaterials* 2001;22(9):943–55.



- [17] Walczak MM, Popenoe DD, Deinhammer RS, Lamp BD, Chung CK, Porter MD. Reductive desorption of alkanethiolate monolayers at gold—a measure of surface coverage. *Langmuir* 1991;7(11):2687–93.
- [18] Imabayashi S, Iida M, Hobara D, Feng ZQ, Niki K, Kakiuchi T. Reductive desorption of carboxylic-acid-terminated alkanethiol monolayers from Au(111) surfaces. *J Electroanal Chem* 1997;428(1–2):33–8.
- [19] Widrig CA, Chinkap C, Porter MD. The electrochemical desorption of n-alkanethiol monolayers from polycrystalline Au and Ag electrodes. *J Electroanal Chem* 1991;310(1–2):335–59.
- [20] Imabayashi S, Hobara D, Kakiuchi T, Knoll W. Selective replacement of adsorbed alkanethiols in phase-separated binary self-assembled monolayers by electrochemical partial desorption. *Langmuir* 1997;13(17):4502–4.
- [21] Yeo WS, Mrksich M. Electroactive self-assembled monolayers that permit orthogonal control over the adhesion of cells to patterned substrates. *Langmuir* 2006;22(25):10816–20.
- [22] Guillaume-Gentil O, Akiyama Y, Schuler M, Tang C, Textor M, Yamato M, et al. Polyelectrolyte coatings with a potential for electronic control and cell sheet engineering. *Adv Mater* 2008;20(3):560–5.
- [23] Takei T, Sakai S, Ono T, Ijima H, Kawakami K. Fabrication of endothelialized tube in collagen gel as starting point for self-developing capillary-like network to construct three-dimensional organs in vitro. *Biotechnol Bioeng* 2006;95(1):1–7.
- [24] Pries AR, Secomb TW, Gaehtgens P. Design principles of vascular beds. *Circ Res* 1995;77(5):1017–23.
- [25] Castagna M, Takai Y, Kaibuchi K, Sano K, Kikkawa U, Nishizuka Y. Direct activation of calcium-activated, phospholipid-dependent protein-kinase by tumor-promoting phorbol esters. *J Biol Chem* 1982;257(13):7847–51.
- [26] Murphy RLW, Smith ME. Effects of diacylglycerol and phorbol ester on acetylcholine-release and action at the neuromuscular-junction in mice. *Br J Pharmacol* 1987;90(2):327–34.
- [27] <http://www.clinicaltrials.gov/ct/show/NCT00004058>.





## Electrochemical desorption of self-assembled monolayers for engineering cellular tissues

Rina Inaba<sup>a</sup>, Ali Khademhosseini<sup>b,c</sup>, Hiroaki Suzuki<sup>a</sup>, Junji Fukuda<sup>a,\*</sup>

<sup>a</sup> Graduate School of Pure and Applied Sciences, University of Tsukuba, 1-1-1 Tennodai, Tsukuba, Ibaraki 305-0006, Japan

<sup>b</sup> Center for Biomedical Engineering, Department of Medicine, Brigham and Women's Hospital, Harvard Medical School, Boston, MA 02115, USA

<sup>c</sup> Harvard-MIT Division of Health Sciences and Technology, Massachusetts Institute of Technology, Cambridge, MA 02139, USA

### ARTICLE INFO

#### Article history:

Received 30 December 2008

Accepted 17 March 2009

Available online 10 April 2009

#### Keywords:

Cell sheet

Spheroid

Fibroblast

Hepatocyte

Self-assembled monolayer

Electrochemistry

### ABSTRACT

Adherent cells, cell sheets, and spheroids were harvested noninvasively from a culture surface by means of electrochemical desorption of a self-assembled monolayer (SAM) of alkanethiol. The SAM surface was made adhesive by the covalent bonding of Arg-Gly-Asp (RGD)-peptides to the alkanethiol molecules. The application of a negative electrical potential caused the reductive desorption of the SAM, resulting in the detachment of the cells. Using this approach greater than 90% of adherent cells detached within 5 min. Furthermore, this approach was used to obtain two-dimensional (2D) cell sheets. The detached cell sheets consisted of viable cells, which could be easily attached to other cell sheets in succession to form a multilayered cell sheet. Moreover, spheroids of hepatocytes of a uniform diameter were formed in an array of cylindrical cavities at a density of 280 spheroids/cm<sup>2</sup> and were harvested by applying a negative electrical potential. This cell manipulation technology could potentially be a useful tool for the fabrication and assembly of building blocks such as cell sheets and spheroids for regenerative medicine and tissue engineering applications.

© 2009 Elsevier Ltd. All rights reserved.

### 1. Introduction

Scaffold-based tissue engineering approaches are beneficial for reconstructing several types of tissue, and have already been used in clinical treatments [1,2]. However, most previous studies have reported abnormalities such as lack of appropriate long-term mechanical and metabolic functions as well as inflammatory responses and fibrosis [3,4]. These are due to mismatches between scaffolds and native matrices, spatial and temporal differences between cell growth and the degradation of scaffolds, a lack of proper vasculature, and the tissue-like organization of different cell types.

One of the potential methods for reconstructing well-organized cell-dense tissues *in vitro* is the use of cellular building blocks. To this end, many attempts have been conducted with microscale cell-laden hydrogels such as collagen and hyaluronic acid [5–7]. Microgels can be either assembled manually or using self-assembling approaches to generate 3-dimensional (3D) tissue constructs. A potential limitation with the use of hydrogels as a cell matrix is that it can result in tissues with decreased cell–cell contact and decreased cell density compared to those observed in native tissues

and organs. An alternative approach to generate tissue building blocks is through the use of cell-dense aggregates such as cell sheets and spheroids [8–10]. For example, a culture surface modified with a thermo-responsive polymer has been used to obtain 2D cell sheets composed of autologous oral mucosal epithelial cells. The sheets have already been used in a clinical trial involving corneal transplantation, which promoted the recovery of weakened vision [11]. However, a drawback is that harvesting a cell sheet typically takes 30–70 min, the rate-limiting step being the hydration of the thermo-responsive polymer on the surface [12,13]. Magnetic beads have also been used to assemble magnetically labeled cells and to form multilayered cell sheets [14]. A magnetic field is applied to collect cells and form a sheet on a non-adherent surface. The cell sheet can be harvested quickly upon removal of the magnetic force. Magnetic beads, however, influence gene expression and have cytotoxic effects depending upon the loading dose [15]. Thus, the development of biocompatible, easily applicable, rapidly collectable approaches is desired for building *in vivo*-like constructs for tissue engineering applications.

In this paper, we present a novel electrochemical method for engineering and harvesting cellular tissues *in vitro* (Fig. 1). In this method, cells are cultured on a self-assembled monolayer (SAM) of alkanethiol. The SAM is reductively desorbed from the gold substrate by the application of a negative electrical potential, which

\* Corresponding author. Tel.: +81 29 853 4995; fax: +81 29 853 4490.  
E-mail address: [fukuda@ims.tsukuba.ac.jp](mailto:fukuda@ims.tsukuba.ac.jp) (J. Fukuda).



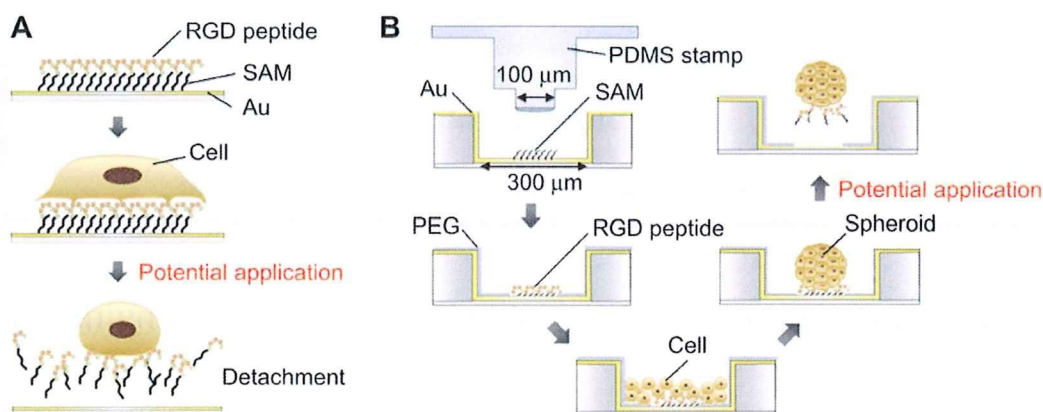


**Fig. 1.** Detachment of cells and spheroids along with the electrochemical desorption of a SAM. (A) The gold surface was first modified with a SAM and a cell-adhesive RGD peptide. Cells on the modified surface were detached by applying  $-1.0$  V. (B) The spheroid culture chip consists of cylindrical cavities at a density of 280 cavities/cm<sup>2</sup>. The central regions (100  $\mu$ m in diameter) at the bottom of the cavities were modified with alkanethiol. The entire region, except the alkanethiol spots, was modified with poly(ethylene glycol) to prevent cell attachment. In the chip, the seeded cells spontaneously formed spheroids, which could be collected by applying a negative potential.

detaches cells and cell sheets from the gold surface in a reliable and rapid manner. The detached cell sheets could be used to form a multilayered cell sheet. Moreover, we applied microfabrication and microcontact printing ( $\mu$ CP) to harvest spheroids. Given its numerous advantages, this technology may be a useful tool for engineering cellular tissues *in vitro*.

## 2. Materials and methods

### 2.1. Materials and reagents

The reagents used for cell culture and tests were purchased from the following commercial sources: Dulbecco's modified Eagle medium (DMEM) and fetal bovine serum (FBS) from Invitrogen, Carlsbad, CA, USA; type I collagen solution from Nitta Gelatin, Osaka, Japan; an ammonia measurement kit, fluorescent diacetate (FDA), and ethidium bromide (EB) from Wako Pure Chemicals industries, Osaka, Japan; goat IgG antibody to rat albumin from LLC-Cappel Products, Durham, NC, USA; rabbit antibody to mouse fibronectin from Novotec, Lyon, France; phosphate buffer saline (PBS)-Tween solution from Calbiochem, La Jolla, CA, USA; fluorescein isothiocyanate (FITC)-labeled mouse anti-goat IgG from Chemicon, Temecula, CA, USA; Qdot 525 goat F(ab') anti-rabbit IgG from Invitrogen, Carlsbad, CA, USA.

Materials used for the fabrication of the culture substrates were obtained from the following commercial sources: glass wafers (#7740, diameter: 76.2 mm, thickness: 500  $\mu$ m) from Corning Japan, Tokyo, Japan; 10-carboxy-1-decanethiol, 7-carboxy-1-heptanethiol, 1-ethyl-3-(3-dimethylaminopropyl)-carbodiimide from Dojindo Laboratories, Kumamoto, Japan; L-cysteine and N-hydroxysuccinimide from Wako Pure Chemicals, Osaka, Japan; GRGDS peptide from Peptide institute, Osaka, Japan; a thick-film photoresist (SU-8) from MicroChem, Newton, MA, USA; liquid prepolymers of poly(dimethylsiloxane) (PDMS) from ShinEtsu Chemical, Tokyo, Japan; poly(ethylene glycol)-SH (PEG-SH, molecular weight 5000; NOF, Tokyo, Japan). All other chemicals were purchased from Sigma, St. Louis, MO, USA, unless otherwise noted.

### 2.2. Adsorption and desorption of SAMs

The adsorption of SAMs was monitored using a quartz crystal microbalance (QCM, Twin-Q; AS ONE, Osaka, Japan). Gold electrodes on the QCM were cleaned with piranha solution ( $\text{H}_2\text{SO}_4:\text{H}_2\text{O}_2$ , 3:1) and 1% sodium dodecyl sulfate. The electrodes were covered with SAMs by immersing them in 1 mM 10-carboxy-1-decanethiol in ethanol, 7-carboxy-1-heptanethiol in ethanol, and 1 mM L-cysteine in water for 30 min at room temperature, respectively. Finally, the QCM was rinsed with each solvent and water and dried. The measurement was performed in air and the frequency change before and after the adsorption of the molecules was compared.

The desorption of the SAMs was performed and analyzed electrochemically [16]. Glass chips (15 mm  $\times$  8 mm) with a gold layer were prepared by sputter-depositing chromium (1 nm) and gold (40 nm). A circular active area (0.4 cm<sup>2</sup>) was delineated on the electrode with a polyimide insulating layer. The surfaces were modified with any of the three thiol molecules mentioned earlier. Then, the substrates were rinsed with each solvent and water. Cyclic voltammograms were obtained with a three-electrode configuration in a 0.5 M KOH solution deoxygenated by bubbling nitrogen gas for 20 min. Electrochemical data were obtained using Autolab (Eco Chemie,

Utrecht, The Netherlands). In this study, all potential values refer to those measured with respect to a Ag/AgCl electrode (#2080 A; Horiba, Tokyo, Japan).

### 2.3. Preparation of cells

Swiss 3T3 murine fibroblasts (RCB1642) were purchased from the Riken Cell Bank, Ibaraki, Japan, and were cultured in DMEM supplemented with 10% FBS. Male Wistar rats weighing approximately 200 g (6–7 weeks old) were purchased from Oriental Bioservice Kanto, Ibaraki, Japan. All animal experiments conformed to the ethical guidelines of the University of Tsukuba. Hepatocytes were isolated from the liver of a rat by perfusion with 0.05% collagenase. Cell viability was assessed using the trypan blue dye exclusion assay, and cells with greater than 85% viability were used for culture. Hepatocytes were cultured in DMEM supplemented with 10 mg/L insulin, 7.5 mg/L hydrocortisone, 50  $\mu$ g/mL epidermal growth factor, 60 mg/L proline, 5 mg/L linoleic acid, 0.1  $\mu$ M  $\text{CuSO}_4$ , 3  $\mu$ g/L  $\text{H}_2\text{SeO}_3$ , 50 pM  $\text{ZnSO}_4$ ,  $1 \times 10^5$  U/L penicillin, 100 mg/L streptomycin, 1.05 g/L  $\text{NaHCO}_3$ , and 1.19 g/L HEPES.

### 2.4. Modification of the surface with SAMs for cell adhesion

To promote the adhesion of cells, the carboxyl terminals of the SAMs were coupled with a cell adhesion peptide through carbodiimide-mediated cross-linking (Fig. 1A). The substrates were immersed in an aqueous solution containing 10 mM 1-ethyl-3-(3-dimethylaminopropyl)-carbodiimide and 10 mM N-hydroxysuccinimide under nitrogen for 30 min at room temperature to convert the carboxyl groups to amine-reactive esters. Immediately after rinsing in water, the esters were reacted with amino groups of the peptide in an aqueous solution of 50  $\mu$ M GRGDS for 1 h. The amount of immobilized RGD peptide was determined with the QCM using the method mentioned in Section 2.2. The substrates were rinsed with 70% ethanol for sterilization and placed in a 35-mm dish. To assess whether the immobilized RGD peptide was bioactive for cell adhesion, fibroblasts ( $1.25 \times 10^5$  cells/ml) suspended in 2 mL of the culture medium containing 1 mM soluble RGD peptide were seeded on the substrate and the number of attached cells were counted after 2 h of culture.

### 2.5. Detachment of single cells

Fibroblasts ( $1.25 \times 10^5$  cells/ml) in 2 mL of the culture medium were seeded on the substrate, and cultured for 12 h at 37  $^\circ$ C in 5%  $\text{CO}_2$  in a humidified incubator. Then, the substrates were washed with PBS three times and connected to a potentiostat (HA-151; Hokuto-Denko, Tokyo, Japan). At 1, 3, and 5 min of the application of  $-1.0$  V, the substrates were washed gently, and the cells that remained on the substrate were counted on phase-contrast micrographs. For comparison, the same experiments were conducted with cells directly attached to a gold surface without the SAMs or when a potential of  $-0.5$  V, which is insufficient to desorb the SAMs, was applied.

### 2.6. Formation of single and multilayered cell sheets

To induce the formation of cell sheets, fibroblasts ( $1.25 \times 10^5$  cells/ml) in 2 mL of the culture medium were seeded on the glass substrates (10 mm  $\times$  10 mm) with a 10-carboxy-1-decanethiol SAM and RGD peptides. The cells were cultured for 3 d until the cells covered the entire surface of the substrate. The cell sheets were detached by applying  $-1.0$  V for 10 min. In forming multilayered cell sheets, a few drops of type I collagen solution (0.24% w/v) were poured onto the first cell sheet and gelled in a humidified incubator for 30 min at 37  $^\circ$ C to facilitate the following



manipulation. Subsequently, the cell sheet covered with a layer of collagen gel was detached from the culture surface, placed on another cell sheet, and incubated for 3 h. The two-layered sheet was again detached from the surface and stacked on another sheet to obtain three-layered cell sheets.

### 2.7. Batch formation of spheroids

The spheroid culture chip was designed to spontaneously form spheroids at the center of each cavity; these spheroids were collected by the application of a negative potential (Fig. 1B). The chip was fabricated by photolithography and  $\mu$ CP [17,18]. Cylindrical cavities of 300- $\mu$ m diameter at a density of 280 cavities/cm<sup>2</sup> were formed with the SU-8 thick-film photoresist. The surface of the chip was covered with a gold layer as in the previous chips. To form a stamp, a master for preparing the PDMS mold was also formed with SU-8. A prepolymer solution composed of a mixture of 10:1 silicone elastomer and the curing agent was poured onto the mold and was cured at 80 °C for 30 min. The cured PDMS sheet was then peeled off from the master and cleaned with ethanol. The PDMS stamp, containing an array of micropillars (100  $\mu$ m in diameter each) was inked with a 10-calboxy-decanthiol solution and was pressed gently onto the center of the bottom of the cavities to form a patterned SAM. The areas surrounding the patterned spots were modified with PEG-SH to prevent cell attachment. The carboxyl terminal of the SAM was coupled with RGD peptides as mentioned earlier. The chip was thoroughly rinsed with distilled deionized water, followed by rinsing in 70% ethanol for sterilization.

The chip was placed in a 35-mm dish, and hepatocytes ( $4 \times 10^5$  cells/ml) in 2.5 mL of the culture medium were seeded. To evaluate the ammonia removal capacity of the hepatocyte spheroids, the culture medium was replaced with a fresh culture medium supplemented with 1 mM ammonium chloride. The ammonia concentration was measured using a commercial kit. The ammonia removal rate ( $\mu$ mol/10<sup>6</sup> cells/day) was calculated from the decrease in ammonia concentration during 24 h after the replacement of the culture medium at predetermined times, and was normalized by the cell number at each time. The cell number was counted as the number of nuclei by using the crystal violet staining method. The nuclei number was converted to the cell number assuming a binuclear ratio of 1:1.45, which had been determined in a preliminary study. For comparison, the same measurements were conducted in a conventional monolayer culture on a type I collagen-coated surface.

### 2.8. Fluorescent and histological staining

Cell growth was monitored using a time-lapse video microscope (IX-71; Olympus, Tokyo, Japan). To identify viable cells in cell sheets and spheroids, dual fluorescent staining was carried out using FDA and EB [19]. FDA stains viable cell cytoplasm green, whereas EB stains dead cell nuclei red. For histological staining, cell sheets were fixed with 3.7% formaldehyde in PBS, embedded in paraffin, and sectioned. Hematoxylin and eosin (H&E) staining was performed following the general procedure. For fluorescent immunostaining, the histological sections were deparaffinized, permeabilized with 0.2% Triton X-100 for 15 min, and treated with 2.0% bovine serum albumin (BSA) for 30 min to block nonspecific adsorption. The sections were then incubated with either goat IgG antibody to rat albumin or rabbit IgG to mouse fibronectin overnight at 4 °C, rinsed with PBS-Tween solution for 15 min, and incubated with FITC-labeled mouse anti-goat IgG or Qdot 525 goat F(ab')<sub>2</sub> anti-rabbit IgG for 1 h at room temperature. Images were taken using a fluorescence microscope (IX-71, Olympus).

## 3. Results and discussion

### 3.1. Adsorption and electrochemical desorption of SAMs

The analysis by QCM revealed that 10-carboxy-1-decanethiol, 7-carboxy-1-heptanethiol, and L-cysteine adsorbed on the electrodes with a density of 0.58 nmol/cm<sup>2</sup>, 0.45 nmol/cm<sup>2</sup>, and 0.38 nmol/cm<sup>2</sup>, respectively. The density of the closely packed monolayer of 10-carboxy-1-decanethiol on Au(111) is estimated to be 0.77 nmol/cm<sup>2</sup> [20]. Therefore, in our case approximately 75% of the maximum amount was adsorbed. The amount of the adsorbed molecules decreased with the decrease in the length of the alkyl chain, which agrees with previous reports [21]. The amount of RGD immobilized on the SAM of 10-carboxy-1-decanethiol was  $88 \pm 28$  pmol/cm<sup>2</sup>, which was sufficiently high for the adhesion of cells since that in typical cases has been  $\sim 20$  pmol/cm<sup>2</sup> at a maximum [22]. Cyclic voltammograms showed a clear dependence of peak potential on the length of the alkyl chain (Fig. 2). With longer chains, the peak potential shifted to the negative direction. The shift has been explained by van der Waals interactions between the alkyl chains

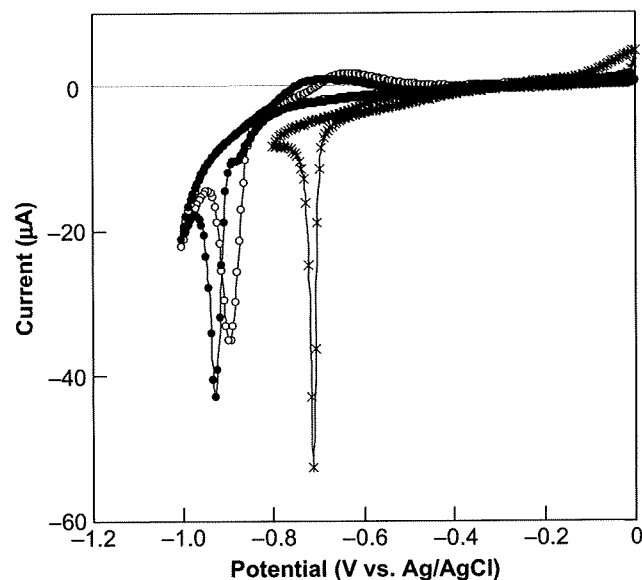


Fig. 2. Cyclic voltammogram observed in the reductive desorption of SAMs. The current peaks for 10-carboxy-1-decanethiol (●), 7-carboxy-1-heptanethiol (○), and L-cysteine (×) were  $-0.93$  V,  $-0.89$  V, and  $-0.71$  V, respectively. Cyclic voltammograms were recorded at a scanning rate of 50 mV/s in a deoxygenated 0.5 M KOH solution with respect to a Ag/AgCl reference electrode. The working electrode area is 0.4 cm<sup>2</sup>.

[23]. Because these peaks were within the range of the electrical potential window of the electrode, we applied  $-1.0$  V for the desorption of all the SAMs in the following experiments.

### 3.2. Separation of single cells from the gold surface

The gold surface modified with SAMs and RGD peptides was used for culturing and collecting cells. Fibroblasts readily attached and spread out on the surface (Fig. 3A). By the inhibition with soluble RGD peptide, the number of attached cells at 2 h of culture was significantly reduced from  $219 \pm 9$  cells/mm<sup>2</sup> to  $39 \pm 16$  cells/mm<sup>2</sup> (the data represent mean  $\pm$  SD of 3 independent experiments), suggesting that the cells were initially recognized and attached through the immobilized peptide. After culturing for 12 h, the cells were detached by applying the potential for 5 min. The cells were gradually detached from the adhesive end and became bright and round after the application of the potential (Fig. 3B). These cells were withdrawn into a micropipette and found to be detached (Fig. 3C).

To quantitatively analyze the detachment of cells, the number of cells that remained on the surface was counted at 1, 3, and 5 min after the application of the potential (Fig. 4). There was no significant difference in the initial number of cells at 12 h of culture among the four conditions (approximately  $3.3 \pm 0.61 \times 10^4$  cells/cm<sup>2</sup>). For the conditions that used the SAMs and an electrical potential of  $-1.0$  V, more than 50% and 95% of the cells detached from the surface within 1 min and 5 min, respectively. On the other hand, few cells detached from a gold surface in the absence of thiol molecules or when the potential was not sufficiently reductive (i.e.,  $-0.5$  V). These results suggest that the detachment occurs mainly due to the electrically dependant desorption of the SAM.

There are a few reports concerning the use of electrochemical approaches for the detachment of cells. SAMs with electroactive sites that respond to electrical potentials have been used for micropatterning of cells by the detachment of cells from a selective region [24]. Although the mechanism of the disruption of the SAMs



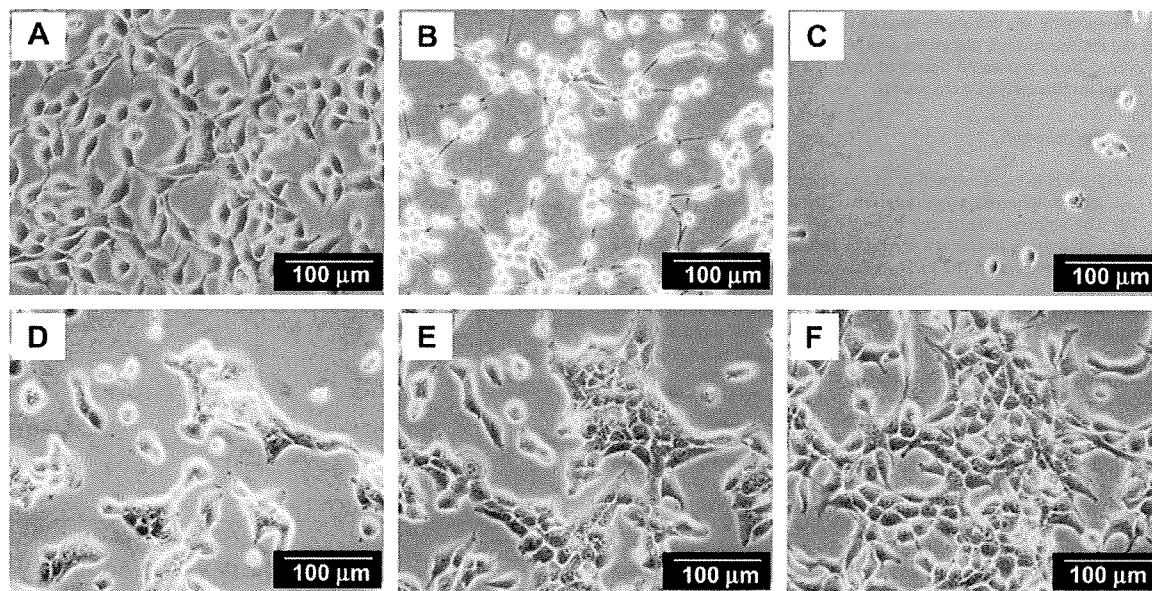


**Fig. 3.** Change in cell morphology before and after the application of the electrical potential. Fibroblasts attached on the gold surface modified with the SAM of 10-carboxy-1-decanethiol and RGD peptide (A). After applying  $-1.0$  V for 5 min, the cells exhibited a bright and round shape (B), and these were identified as being detached after gentle pipetting (C). Detached cells reattached and proliferated at 6 h (D), 12 h (E), and 24 h (F) after the application of the potential.

is not exactly the same as in our case, cells were detached within several minutes, which is compatible with our observations. On the other hand, other stimuli such as temperature changes have been used for the detachment of cells [25]. In a surface modified with

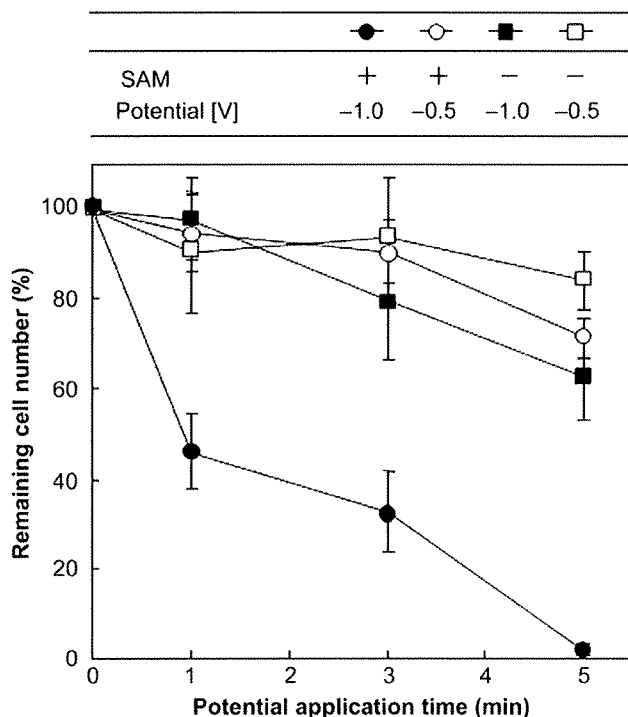


**Fig. 4.** Change in the number of cells remaining on the gold surfaces. Fibroblasts were attached on the gold surfaces with and without the SAM of 10-carboxy-1-decanethiol and RGD peptide, and potentials of  $-1.0$  V and  $-0.5$  V were applied. More than 90% of the cells were detached within 5 min along with the desorption of the SAM for  $-1.0$  V studies, whereas cells were not detached in the other three cases. The error bars indicate SD calculated from at least 3 independent experiments for each plot.

a thermo-responsive polymer, an incubation of longer than 50 min was necessary to detach more than 90% of the cells [13]. Although this time period was shortened by optimizing substrate structures and the ratio of co-grafting polymers, it still required 20–30 min [12]. This point appears to be particularly critical when the process is repeated a number of times for building up 3D cellular tissues. In addition, its widespread use is prevented since the method requires specialized devices for grafting thermo-responsive polymers and for maintaining the temperature at  $37$  °C for preventing the undesired detachment of cells throughout the culture. Our method only requires commercially available materials, reagents, and an electric source such as a cell battery, thereby facilitating the utilization of the method in biological and medical laboratories and industries.

To examine the viability of the detached cells, the cells were left undisturbed and grown. These cells spread again on the surface and proliferated vigorously (Fig. 3D–F), indicating that the potential did not exert a serious adverse influence on the cells. Others have also shown that the application of a negative potential does not cause any serious adverse influence on the cells when cells were grown in a cell-inert region that was modified with oligoethylene glycol-terminated SAMs after its electrochemical desorption; however, that study did not intend to detach cells and used a relatively high potential for a short time period ( $-1.2$  V for 30 s) [26]. Although we conducted experiments with three different thiolated molecules, no significant difference was observed. Considering the fact that the cells detached gradually from the adhesive end, the rate-limiting process appears not to be the electrical desorption of SAMs but the dynamic behavior of cells such as contraction of the cell membrane during the detachment. Therefore, we used 10-carboxy-1-decanethiol for the remainder of our studies. In combinations of two thiol molecules, it has been noted that phase-separated binary SAMs are formed on a gold surface and the domains of the molecule with the lower negative desorption potential are selectively removed by controlling the potential of the surface [27]. It remains to be seen whether such nanoporous SAM surfaces can be effectively used in our method for a more rapid processing.

### 3.3. Detachment of cell sheets

2D cell sheets were also detached from the surface by the application of a negative potential. Fibroblasts were cultured on the gold substrate with 10-carboxy-1-decanethiol and RGD peptide and grown to confluence for 3 d. Application of  $-1.0$  V to the surface caused detachment of a single-layered cell sheet ( $10\text{ mm} \times 10\text{ mm}$ ) within 10 min (Fig. 5A). FDA/EB staining showed that all the cells in the harvested cell sheet were viable (Fig. 5B). Unlike cells collected by treatment with proteinase such as trypsin or collagenase, the cell sheet is expected to be harvested together with extracellular matrix (ECM) molecules that are deposited during the culture and intact cell membrane proteins such as gap junctions and growth factor receptors. Fluorescent immunostaining indicated that fibronectin still remained in the sheet after the detachment (Fig. 5C). Although there is a possibility that alkanethiol molecules also remain bound in cell membrane proteins of the detached cells, because ECM molecules accumulate between the cell sheet and substrate during culture and have significantly larger molecular sizes compared with alkanethiol molecules, cells may increasingly become attached to ECM molecules rather than alkanethiol molecules over time. The presence of ECM molecules enhances the expression of tissue-specific functions as well as allows for stacking on another cell sheet and subsequent adhesion to host tissues, as reported in cell sheets formed by using thermo-sensitive polymer-grafted surfaces [25]. To our knowledge, this is the first report concerning the use of electrochemical desorption of a SAM to collect 2D cell sheets.

### 3.4. Multilayered cell sheets

We successfully constructed multilayered sheets of fibroblasts or hepatocytes by stacking harvested cell sheets one by one. One of the harvested cell sheets was placed on another confluent monolayer. The cell sheets spontaneously adhered to each other. We then stacked the double-layered sheet on another sheet and fabricated triple-layered cell sheets. The process can be repeated to obtain multilayered cell sheets. As shown in Fig. 5E and F, cell sheets ( $10\text{ mm} \times 10\text{ mm}$ ) formed three-layered tissues with close cell–cell

connections. The single-layered hepatocyte sheet was approximately  $10\text{ }\mu\text{m}$  in thickness (Fig. 5D), which increased to  $30\text{--}40\text{ }\mu\text{m}$  in thickness (Fig. 5E) for the three-layered sheet. Hepatocytes in the stacked sheet had a cuboidal cell shape, unlike the conventional monolayer culture in which cells exhibit an extended shape. The shape of hepatocytes is closely related to the maintenance of their functions *in vitro* [28]. Hepatocytes in the three-layered sheet maintained one important liver-specific function, i.e., albumin secretion, even after stacking and 4 d of culture (Fig. 5F). Although we left the cell sheets to be attached for a relatively long time period of 3 h in this study, the processing time should be as short as possible in constructing cell sheets with more layers. The time may depend on the type of cells, the size of cell sheets, and the method used for harvesting the cell sheets. In the studies that used a thermo-responsive polymer surface, cardiac cell sheets were attached to each other in the order of minutes [29]. These points are the focus of our future investigations.

### 3.5. Spheroid formation and detachment

It is well known that spheroid morphology is preferred for the maintenance and culture of specific cell types including hepatocytes, probably due to close cell–cell interactions and cuboidal shapes as mentioned above. Hepatocytes that are cultured in non-adhesive dishes form 3D aggregates and maintain their specific functions better than those in a 2D monolayer culture [30]. Here, we fabricated the chip for the formation and collection of spheroids (Fig. 1B). Hepatocytes inoculated in the chip entered each cavity, gathered at the center of the cavity at 12 h of culture, and spontaneously formed spheroids on the cell adhesion regions within 3 d of culture (Fig. 6A and B). The spheroids had a smooth surface and consisted of indistinct individual cells (Fig. 6C).

Spheroids of uniform diameter formed in almost all the cavities at a density of  $280$  spheroids/ $\text{cm}^2$  (Fig. 6D). The diameter of the spheroids was  $178 \pm 6\text{ }\mu\text{m}$  (mean  $\pm$  SD), which was calculated from the image analyses of 10 micrographs in 3 independent preparations of the liver. In large spheroids, cell necrosis occurs within the core of the spheroids since surface diffusion is the only means of oxygen supply

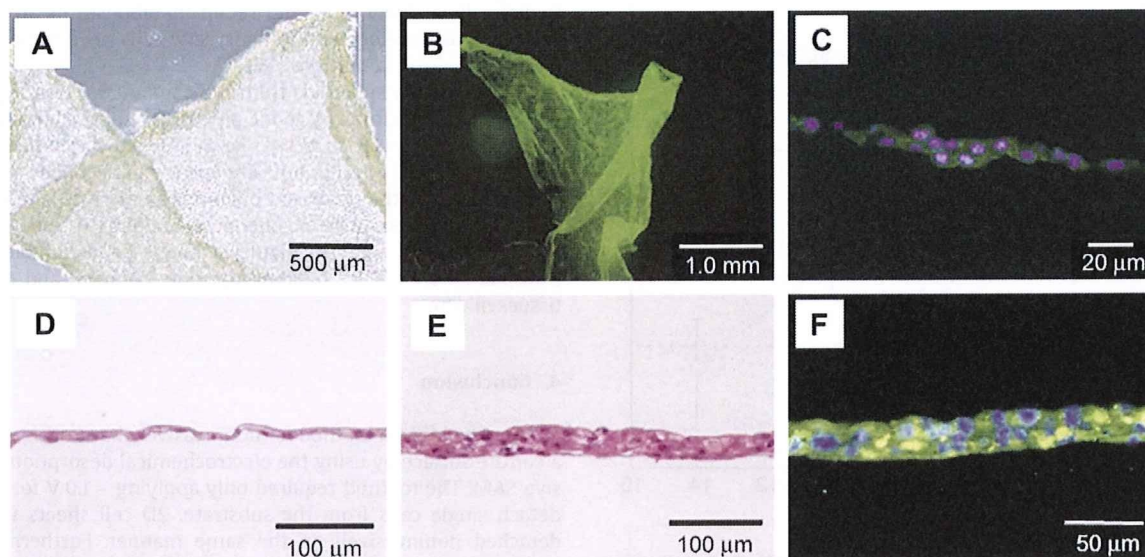


**Fig. 5.** Cell sheets and multilayered cell sheets. A monolayer fibroblast sheet was electrochemically harvested (A). The live/dead fluorescent staining of the fibroblast sheet demonstrates that the majority of cells in the sheet are alive (green) with only a few dead cells (red) (B). Fluorescent staining of fibronectin (green) and nuclei (blue) in the cross-section revealed that the detached fibroblasts contained ECM in the sheet (C). A single layer (D) and a three-layered hepatocyte sheet (E) were sectioned and stained with H&E. Fluorescently stained albumin (green) and nuclei (blue) in the cross-section of a three-layered hepatocyte sheet (F).



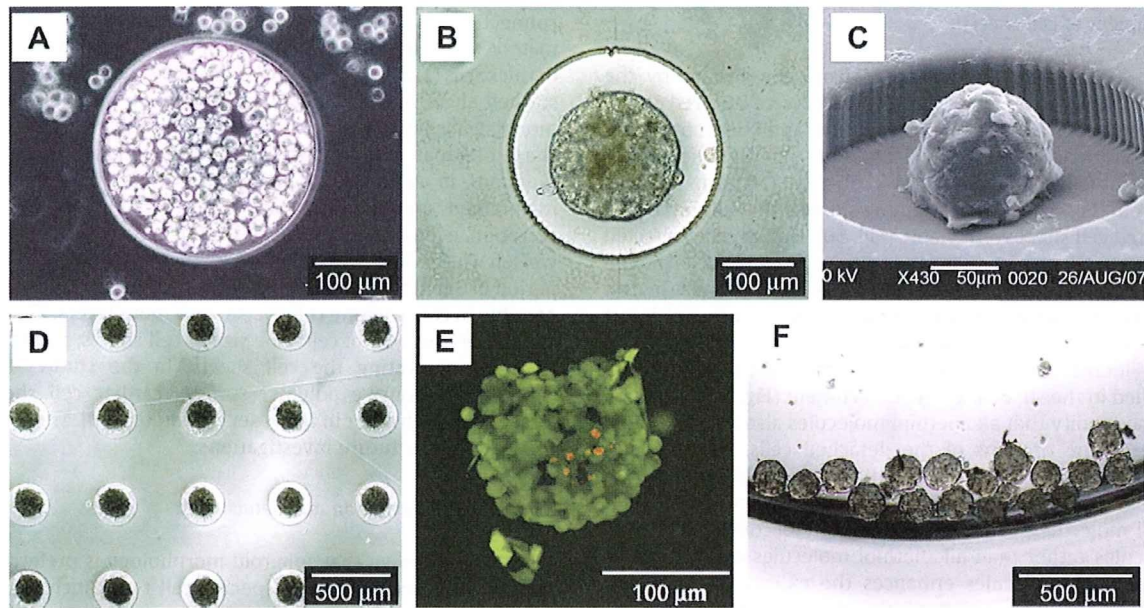


**Fig. 6.** Hepatocyte spheroids in the microfabricated chip. Hepatocytes seeded on the chip were inserted in the cavities (A), which spontaneously formed a spheroid in the cavity within 3 d of culture (B). Scanning electron micrograph of a spheroid (C). The spheroids had a uniform diameter at the center of each cavity (D). The live/dead fluorescent assay using confocal microscopy shows that the cells in the spheroid were nearly all viable with only a few dead cells in the core of the spheroid (E). The spheroids were harvested by the application of a potential of  $-1.0$  V (F).

due to the absence of blood vessels. Therefore, the uniform regulation of the size of tissue constructs is one of the major issues in tissue engineering. The diameter of a spheroid at the survival limit has been mathematically and experimentally calculated to be in the range of  $100\text{--}200\ \mu\text{m}$  [31,32]. The conditions for the survival of hepatocytes in the spheroids in the chip were investigated by FDA/EB staining (Fig. 6E). Almost all the cells in the spheroids were viable, with only a few dead cells in the core of the spheroids. The chip culture system allows us to control the size of spheroid diameters by changing

system parameters such as the cavity diameter, stamp diameter, and inoculation cell number. These abilities may contribute to the estimation of the survival limit diameter of a spheroid in various conditions and to obtain new types of biological knowledge, such as the manner in which several cells need to express tissue-specific phenotypes or the relationship between cell aggregate sizes and cell-cell communication.

The spheroids stably retained their conformation and liver-specific function of ammonia removal for at least 14 d of culture (Fig. 7). On the other hand, hepatocytes cultured in a conventional monolayer in type I collagen-coated dishes, rapidly lost the function after 7 d. While some cell types such as fibroblasts and endothelial cells actively grow and retain metabolism in 2D cultures, cells such as hepatocytes and pancreatic cells need to be cultured under 3D culture conditions [33,34].

To harvest the spheroids from the chip,  $-1.0$  V was applied for 10 min at 3 d of culture. By gentle pipetting, almost all the spheroids in the chip were easily collected (Fig. 6F). Hepatocyte spheroids have been transplanted intraperitoneally, and their effectiveness has been demonstrated in the treatment of animals with liver failure despite a wide distribution range of spheroid diameters [9]. Spheroids with a controlled and uniform diameter might be preferable for cell transplantation and for building up more complex and organized tissues *in vitro*.

#### 4. Conclusion

We developed a method for noninvasively harvesting cells from a culture surface by using the electrochemical desorption of adhesive SAM. The method required only applying  $-1.0$  V for 5 min to detach single cells from the substrate. 2D cell sheets were also detached noninvasively in the same manner. Furthermore, the detached cell sheets adhered to other identical cell sheets in succession to form a multilayered cell sheet. The method could also be used to harvest spheroids by the combination of microfabrication and  $\mu\text{CP}$ . An unresolved issue of our method is that alkanethiol

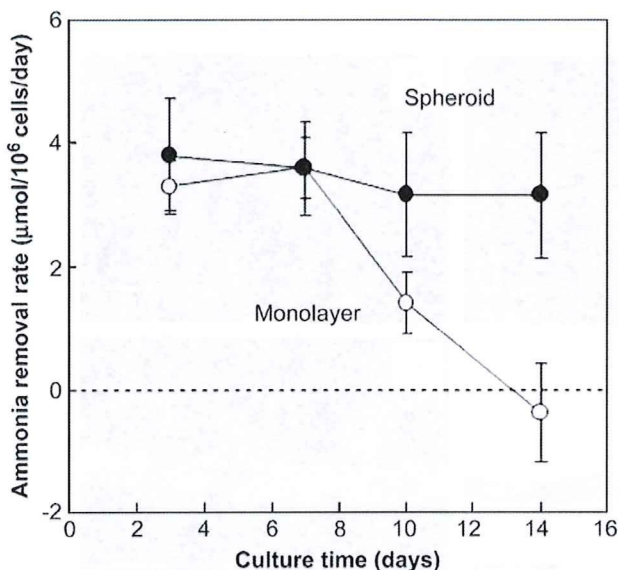


**Fig. 7.** Ammonia removal rate. Hepatocytes in the spheroid culture on the chip maintained ammonia removal function for at least 14 d of culture, whereas hepatocytes in the monolayer culture on a collagen-coated dish rapidly lost the function after 7 d of culture. The error bars indicate SD calculated from 9 experiments from 3 independent preparations of the liver.

molecules may remain bound in the cell membrane proteins of the detached cells. Although we have not examined whether the molecules would cause any inflammatory responses in the body after transplantation, no adverse influence on the detached cells was demonstrated. It is noteworthy that cysteine could be used in our approach. Thus, as an alternative, natural or synthetic oligopeptides which contain cysteine and RGD may also be used in our approach. This electrochemical technology could potentially be a useful tool for the fabrication and assembly of such building blocks for regenerative medicine and tissue engineering applications.

### Acknowledgements

This research has been supported by MEXT (Grant-in-Aid for Young Scientists (A), 20686056), Ministry of Health, Labour and Welfare (H20-Saisei-wakate-010), NEDO (Industrial Technology Research Grant Program, 06A06014a).

### References

- [1] Atala A, Bauer SB, Soker S, Yoo JJ, Retik AB. Tissue-engineered autologous bladders for patients needing cystoplasty. *Lancet* 2006;367(9518):1241–6.
- [2] Park H, Cannizzaro C, Vunjak-Novakovic G, Langer R, Vacanti CA, Farokhzad OC. Nanofabrication and microfabrication of functional materials for tissue engineering. *Tissue Eng* 2007;13(8):1867–77.
- [3] Ronneberger B, Kao WJ, Anderson JM, Kissel T. In vivo biocompatibility study of ABA triblock copolymers consisting of poly(L-lactic-co-glycolic acid) A blocks attached to central poly(oxyethylene) B blocks. *J Biomed Mater Res* 1996;30(1):31–40.
- [4] Sung HJ, Meredith C, Johnson C, Galis ZS. The effect of scaffold degradation rate on three-dimensional cell growth and angiogenesis. *Biomaterials* 2004;25(26):5735–42.
- [5] Khademhosseini A, Eng G, Yeh J, Fukuda J, Blumling 3rd J, Langer R, et al. Micromolding of photocrosslinkable hyaluronic acid for cell encapsulation and entrapment. *J Biomed Mater Res A* 2006;79(3):522–32.
- [6] Khademhosseini A, Langer R. Microengineered hydrogels for tissue engineering. *Biomaterials* 2007;28(34):5087–92.
- [7] Du Y, Lo E, Ali S, Khademhosseini A. Directed assembly of cell-laden microgels for fabrication of 3D tissue constructs. *Proc Natl Acad Sci USA* 2008;105(28):9522–7.
- [8] Fukuda J, Khademhosseini A, Yeo Y, Yang X, Yeh J, Eng G, et al. Micromolding of photocrosslinkable chitosan hydrogel for spheroid microarray and co-cultures. *Biomaterials* 2006;27(30):5259–67.
- [9] Hamazaki K, Doi Y, Koide N. Microencapsulated multicellular spheroid of rat hepatocytes transplanted intraperitoneally after 90% hepatectomy. *Hepatology* 2002;49(48):1514–6.
- [10] Ohashi K, Yokoyama T, Yamato M, Kuge H, Kanehiro H, Tsutsumi M, et al. Engineering functional two- and three-dimensional liver systems in vivo using hepatic tissue sheets. *Nat Med* 2007;13(7):880–5.
- [11] Nishida K, Yamato M, Hayashida Y, Watanabe K, Yamamoto K, Adachi E, et al. Corneal reconstruction with tissue-engineered cell sheets composed of autologous oral mucosal epithelium. *N Engl J Med* 2004;351(12):1187–96.
- [12] Hyeon Kwon O, Kikuchi A, Yamato M, Okano T. Accelerated cell sheet recovery by co-grafting of PEG with PIPAAm onto porous cell culture membranes. *Biomaterials* 2003;24(7):1223–32.
- [13] Kwon OH, Kikuchi A, Yamato M, Sakurai Y, Okano T. Rapid cell sheet detachment from poly(N-isopropylacrylamide)-grafted porous cell culture membranes. *J Biomed Mater Res* 2000;50(1):82–9.
- [14] Ito A, Ino K, Kobayashi T, Honda H. The effect of RGD peptide-conjugated magnetite cationic liposomes on cell growth and cell sheet harvesting. *Biomaterials* 2005;26(31):6185–93.
- [15] Tiwari A, Punshon G, Kidane A, Hamilton G, Seifalian AM. Magnetic beads (Dynabead) toxicity to endothelial cells at high bead concentration: implication for tissue engineering of vascular prosthesis. *Cell Biol Toxicol* 2003;19(5):265–72.
- [16] Walczak MMPD, Deinhammer RS, Lamp BD, Chung CK, Porter MD. Reductive desorption of alkanethiolate monolayers at gold – a measure of surface coverage. *Langmuir* 1991;7(11):2687–93.
- [17] Fukuda J, Sakai Y, Nakazawa K. Novel hepatocyte culture system developed using microfabrication and collagen/polyethylene glycol microcontact printing. *Biomaterials* 2006;27(7):1061–70.
- [18] Whitesides GM, Ostuni E, Takayama S, Jiang X, Ingber DE. Soft lithography in biology and biochemistry. *Annu Rev Biomed Eng* 2001;3:335–73.
- [19] Gray DW, Morris PJ. The use of fluorescein diacetate and ethidium bromide as a viability stain for isolated islets of Langerhans. *Stain Technol* 1987;62(6):373–81.
- [20] Widrig CA, Chung C, Porter MD. The electrochemical desorption of n-alkanethiol monolayers from polycrystalline Au and Ag electrodes. *J Electroanal Chem* 1991;310(1–2):335.
- [21] Zhang JCQ, Nielsen JU, Friis EP, Andersen JET, Ulstrup J. Two-dimensional cysteine and cystine cluster networks on Au(111) disclosed by voltammetry and in situ scanning tunneling microscopy. *Langmuir* 2000;16(18):7229–37.
- [22] Houseman BT, Mrksich M. The microenvironment of immobilized Arg-Gly-Asp peptides is an important determinant of cell adhesion. *Biomaterials* 2001;22(9):943–55.
- [23] Imabayashi S, Iida M, Hobara D, Feng ZQ, Niki K, Kakiuchi T. Reductive desorption of carboxylic-acid-terminated alkanethiol monolayers from Au(111) surfaces. *J Electroanal Chem* 1997;428(1–2):33–8.
- [24] Yeo WS, Mrksich M. Electroactive self-assembled monolayers that permit orthogonal control over the adhesion of cells to patterned substrates. *Langmuir* 2006;22(25):10816–20.
- [25] Yamato M, Akiyama Y, Kobayashi J, Yang J, Kikuchi A, Okano T. Temperature-responsive cell culture surfaces for regenerative medicine with cell sheet engineering. *Prog Polym Sci* 2007;32(8–9):1123.
- [26] Jiang X, Ferrigno R, Mrksich M, Whitesides GM. Electrochemical desorption of self-assembled monolayers noninvasively releases patterned cells from geometrical confinements. *J Am Chem Soc* 2003;125(9):2366–7.
- [27] Imabayashi S, Hobara D, Kakiuchi T, Knoll W. Selective replacement of adsorbed alkanethiols in phase-separated binary self-assembled monolayers by electrochemical partial desorption. *Langmuir* 1997;13(17):4502–4.
- [28] Berthiaume F, Moghe PV, Toner M, Yarmush ML. Effect of extracellular matrix topology on cell structure, function, and physiological responsiveness: hepatocytes cultured in a sandwich configuration. *FASEB J* 1996;10(13):1471–84.
- [29] Shimizu T, Yamato M, Isoi Y, Akutsu T, Setomaru T, Abe K, et al. Fabrication of pulsatile cardiac tissue grafts using a novel 3-dimensional cell sheet manipulation technique and temperature-responsive cell culture surfaces. *Circ Res* 2002;90(3):e40.
- [30] Fukuda J, Nakazawa K. Orderly arrangement of hepatocyte spheroids on a microfabricated chip. *Tissue Eng* 2005;11(7–8):1254–62.
- [31] Fukuda J, Okamura K, Nakazawa K, Iijima H, Yamashita Y, Shimada M, et al. Efficacy of a polyurethane foam/spheroid artificial liver by using human hepatoblastoma cell line (Hep G2). *Cell Transplant* 2003;12(1):51–8.
- [32] Glicklis R, Merchuk JC, Cohen S. Modeling mass transfer in hepatocyte spheroids via cell viability, spheroid size, and hepatocellular functions. *Bio-technol Bioeng* 2004;86(6):672–80.
- [33] Hober C, Benhamou PY, Watt PC, Watanabe Y, Nomura Y, Stein E, et al. A new culture method for human pancreatic islets using a biopore membrane insert. *Pancreas* 1997;14(2):199–204.
- [34] Nakazawa K, Izumi Y, Fukuda J, Yasuda T. Hepatocyte spheroid culture on a polydimethylsiloxane chip having microcavities. *J Biomater Sci Polym Ed* 2006;17(8):859–73.



